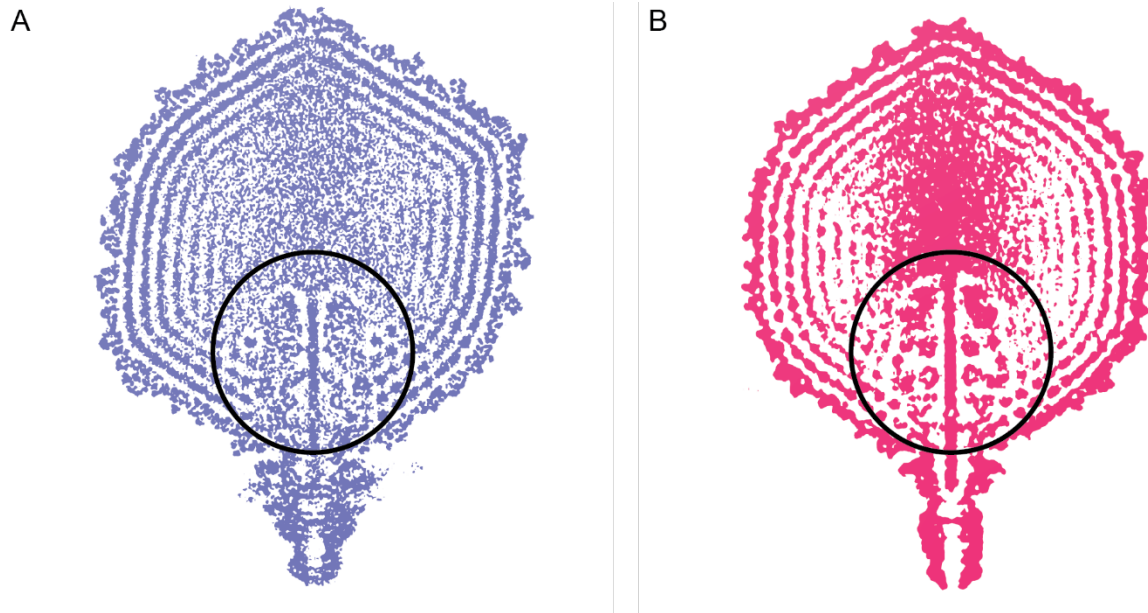


1

**Supplementary file**



2

3 **Supplementary Figure 1: HRP29 has an inner core, related to Figure 1.**

4 (A) Central slice from the asymmetric reconstruction of HRP29 (EMD – 28227) colored in blue

5 and the inner stack highlighted by the circle. (B) Central slice from the symmetry mismatch

6 reconstruction of T7 (EMD – 31315) colored in pink and the inner stack highlighted by the circle.

7

8

9

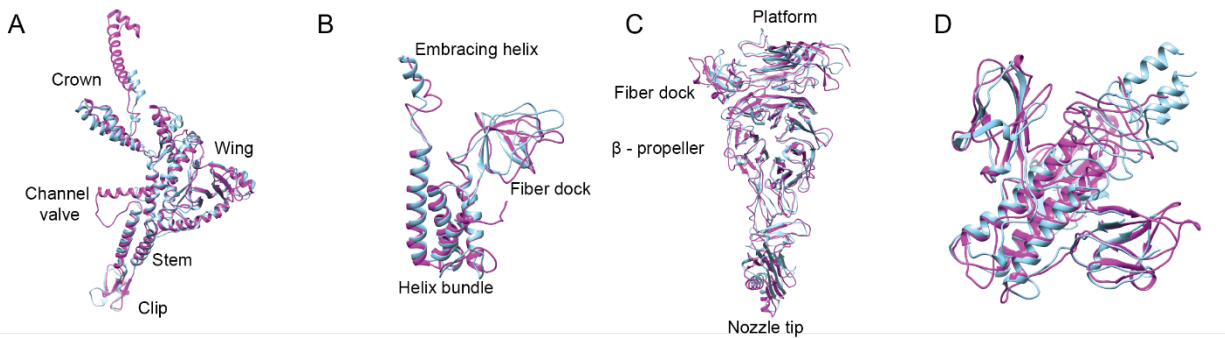
10

11

12

13

14



15

16 **Supplementary Figure 2: Comparison of individual tail protein structures, related to Figure**

17 **2.** (A) Portal gp35 from HRP29 (blue) and gp8 from T7 (pink) were aligned against each other  
 18 with a RMSD of 1.078 Å. (B) Adaptor gp39 from HRP29 and gp11 from T7 were aligned against  
 19 each other with a RMSD of 1.068 Å. (C) Nozzle gp40 from HRP29 and gp12 from T7 were aligned  
 20 against each other with a RMSD of 1.312 Å. (D) Tailspike adaptor gp44 from HRP29 and gp17  
 21 from T7 were aligned against each other with a RMSD of 1.160 Å.

22

23

24

25

26

27

28

29

30

31

32

33

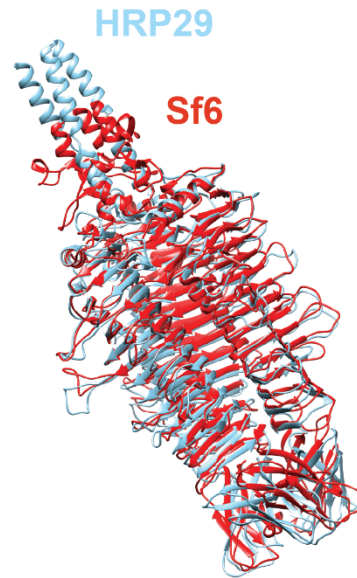
34

35

A

<i>HRP29</i>	1	MTDIIITNVVIGMPSQLFTMAR5FKAVANGKIYIGKIDTDPVNPENQIQVYVENEDGSHVPVSQPIVINAAGYPVYNGQIA
<i>Sf6</i>	1	-----MAAVSSLTKLIRORAQNVTYNSTN-----VQAQLDSLPIW5LADPR---
<i>HRP29</i>	81	KFVTEQGH5MAVYDAYGSQFYFQNVLYKYPDQFGPDLIEQLAQSGKYSQDNTKGDAMIQVVKQPLKAVLRTQHDKNKEA
<i>Sf6</i>	81	-----WGADATGATDSTARIQACFNIVGS-RGGGTVYIPATPGDGAANNQ---GYKVS6SIEVPFVNIQGEF55SCLRA
<i>HRP29</i>	161	ISILDVGVDDGVTQNYQAIQNAIDAVASLPSGGELFIPAS-----NQAVGYIVG5TLLIPGGVNIIRGVGKASQLRA
<i>Sf6</i>	161	-----KSLTGSVLR5L5D5DTIGRYLRNIRVTGNNTGNGIDTNI5AEDSVIRQVYGVWFDNV5MNEVETAYLMQGLW5KFIAC
<i>HRP29</i>	194	TTSACRVGLHLWGQNV5INILGSHFRDR5DRDKDTFGIVIQPRVYAW5PQTRGR5RSETIVMGGEFMCI5QEYGIYVHDV
<i>Sf6</i>	194	QAGTCRVGLHL5GQCV5V555CHFSRGNYSAD5E5FGIRIQPQTYAW55EAVR---SEAIILD5ETMCI5GF5NAV5YVHDC
<i>HRP29</i>	274	LDLQISNMDL5YIFLIAIAIILNVNGG5NISDGNIAAD5TGTQF5GIVFANPLD5VQ5MKT5VRGL5HNL5ANN5PLANN5QV
<i>Sf6</i>	274	LDLHMEQLD5L5YCG5TG5V5I5EN5VGG5F5FS5NS5WIAAD5AD5GTEQ5FTGIYFRTPT5TQ5HKI5V5GVH5INT5ANK5TAANN5QSI
<i>HRP29</i>	354	AIASQK5VK5VAIRDCT5F5GGW5AG5VDI5QNT5AG5IID5GNI5FAGNT5LSLR5SGH5VTIT5NRL5DN5VTETGK---AAVNT5MG5N
<i>Sf6</i>	354	AIEQ5SAIF-VF5VSG5CTL5GDEW5AVNI5VDINECV5FDK5CIFNK5PLR5LRS5G--V5VTD5CYLAGITEVQ5KPEGR5NTYR5GCS
<i>HRP29</i>	432	NGKFTD5GIVQ5VMPAS5NS5GL5QLPNP5VAGAT5YVAEL5MG5N5SAQ5T5SDF5AVEG5SV5R5RAT5PV5AV5LV5R5VTML 508
<i>Sf6</i>	432	GVPSVNGI5INVP5AVGAT5G5SAAI5PNP--GNL5TYR5V5R5L5FG5P5ASS5G5K5V5S5G5VT5INV5TR5P5PV5G5AL5PSM5VE5LAI 623

B



37

38 Supplementary Figure 3: Comparison of HRP29 tailspike and Sf6 tailspike, related to Figure

39 **2.** (A) Sequence alignment of HRP29 tailspike gp52 and Sf6 tailspike gp14 using BLAST.

40 Conserved catalytic residues Glutamate 366 and Aspartate 399 are highlighted in a red box. (B)

41 An AlphaFold prediction of gp52 trimer was aligned with the crystal structure of Sf6 tail spike (PDB:

42 2VBM) in chimera (RMSD: 0.899Å).

43

44

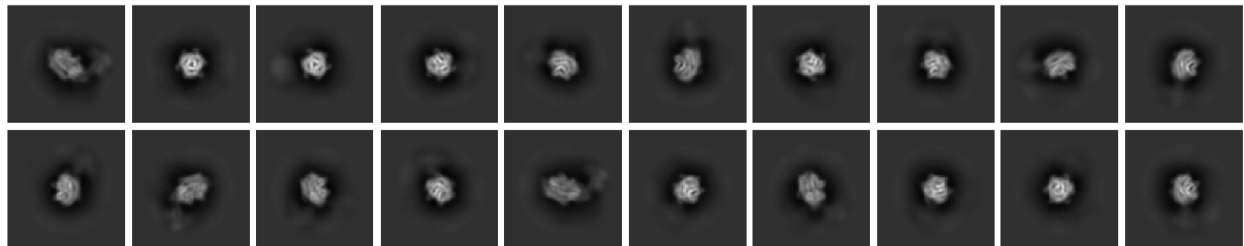
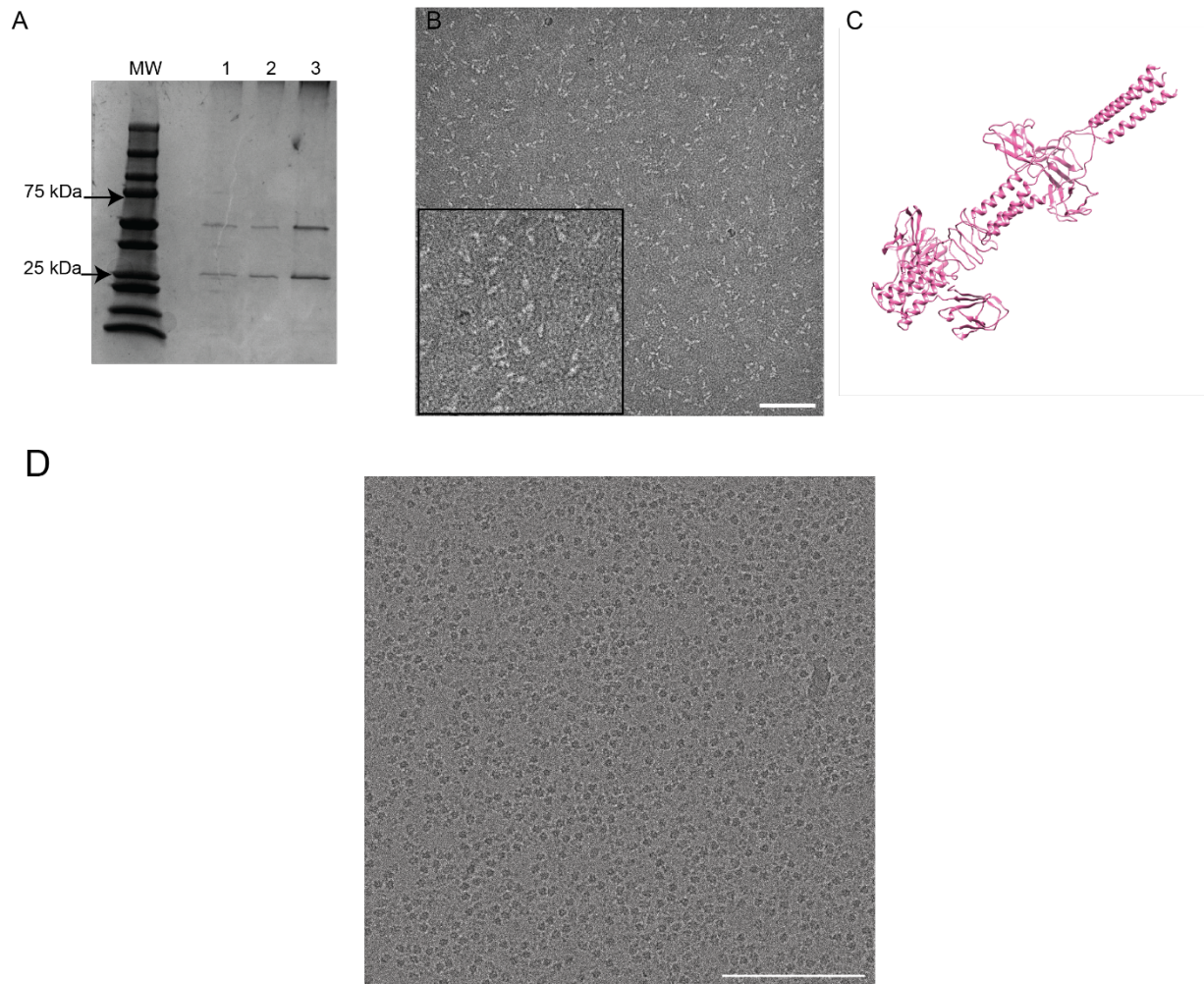
45

46

47

48

49



50

51 Supplementary Figure 4: gp44-gp52 SDS PAGE, gp44-gp52 complex negative stain image,

52 **gp44 alphafold prediction and gp44-gp52 cryo-EM, related to Figure 3.** (A) SDS-PAGE gel

53 of size exclusion chromatography fractions of gp44-gp52 complex. First lane is molecular weight

54 marker and lanes 1, 2, and 3, are fractions from the size exclusion chromatography. (B)

55 Micrograph of negatively stained gp44-gp52 complex along with a zoomed in view. Scale bar is

56 100 nm. (C) Alphafold prediction of gp44 trimer. (D) Micrograph of gp44-gp52 complex in vitreous  
57 ice. Micrographs were collected using a Talos Arctica equipped with a Falcon 3 direct electron  
58 detector operating in counting mode. Scalebar is 100 nm. (E) 2D class averages of particles from  
59 several micrographs showing predominantly top views and side views with no clear density for  
60 gp44.

61

62

63

64

65

66

67

68

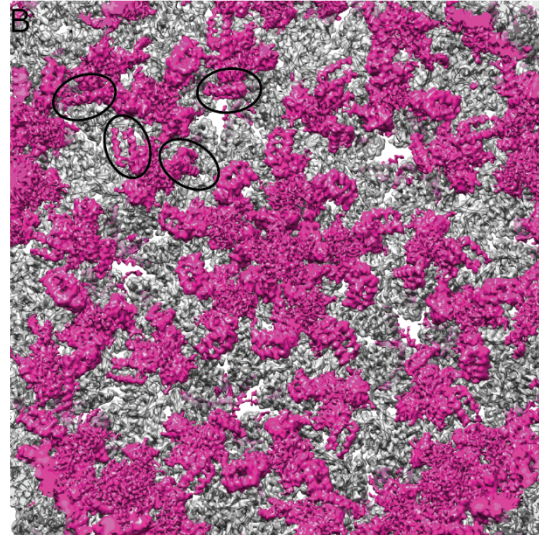
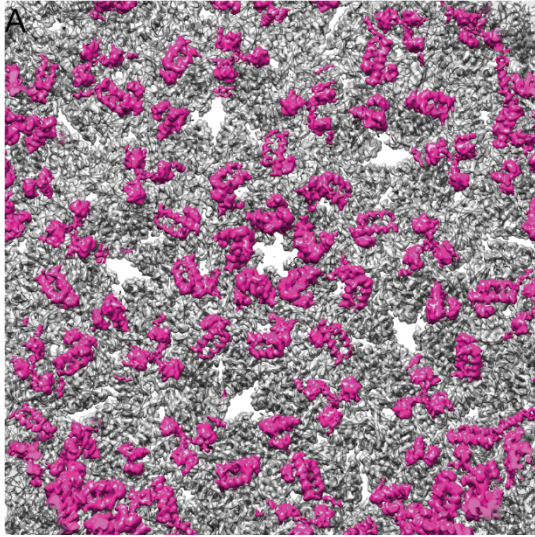
69

70

71

72

73



74

75 Supplementary Figure 5: HRP29 procapsid has scaffolding protein density just beneath the

76 **N-terminus, related to Figure 6.** (A) Interior view of the procapsid with the capsid density colored

77 in grey and the scaffolding density from the difference map colored in magenta. The difference

78 map was calculated by subtracting the map generated from the icosahedral model and the original

79 map, both calculated at 3.5 Å. (B) Same interior view from (A) but the difference map is contoured

80 at a lower value to show weaker densities that are highlighted by black circles.

81

82

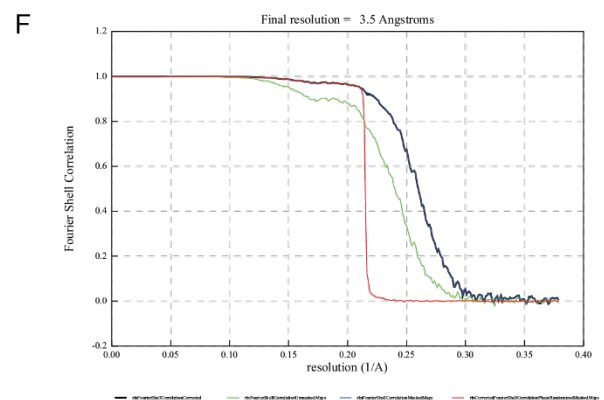
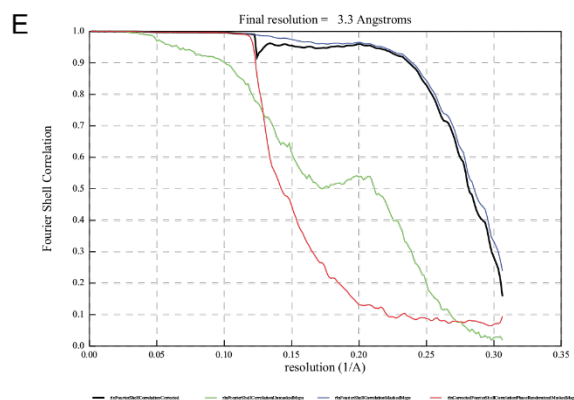
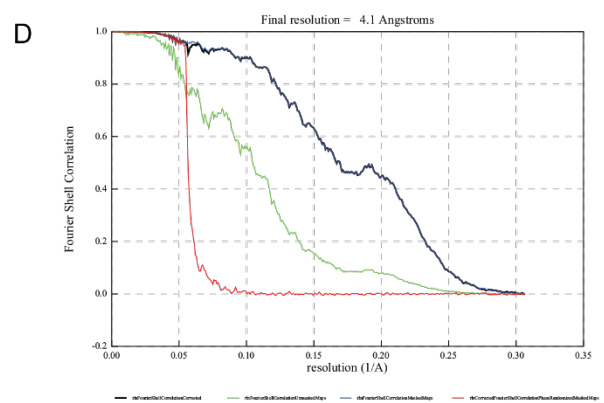
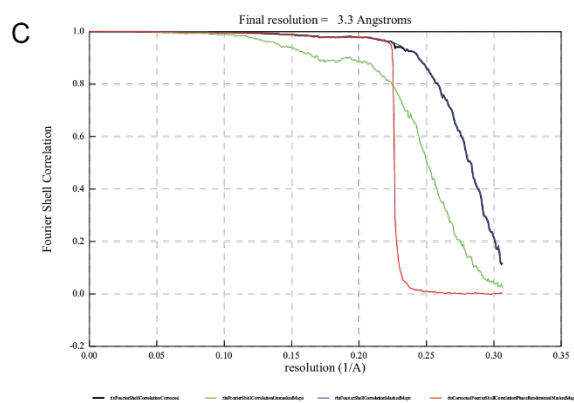
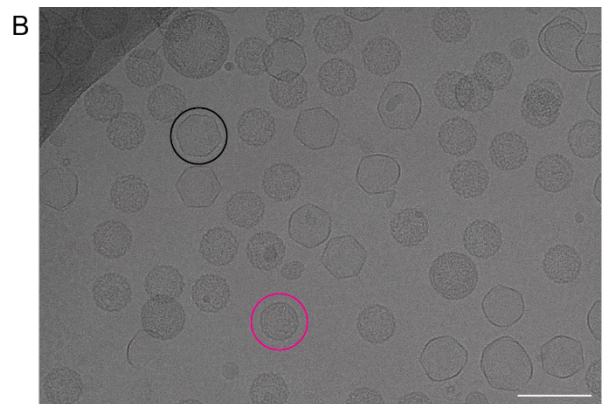
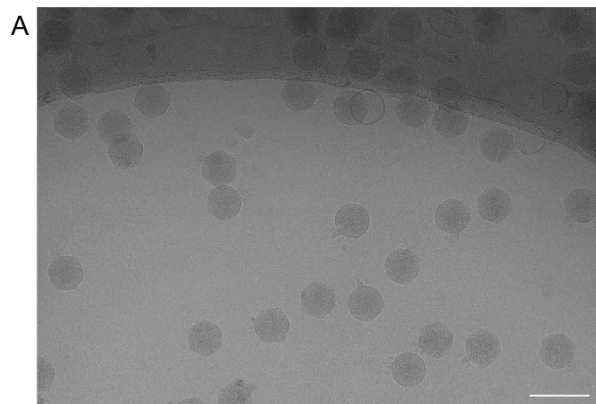
83

84

85

86

87



88

89 **Supplementary Figure 6: Raw micrographs after motion correction and FSC curves, related**  
 90 **to STAR methods.** (A) Micrograph of HRP29 virions after motion correction. (B) Micrograph of  
 91 HRP29 procapsids after motion correction. A representative procapsid highlighted by pink circle  
 92 and expanded head highlighted by black circle. Scale bar is 100 nm. (C) FSC curve from the  
 93 icosahedral reconstruction of HRP29 virions. (D) FSC curve from the asymmetric reconstruction

94 of HRP29 virions. (E) FSC curve from the focused C6 reconstruction of HRP29 tail. (F) FSC curve  
 95 from the icosahedral reconstruction of HRP29 procapsids.

96  
 97

98 **Supplementary Table1: EOP of HRP29 on various mutants, related to STAR methods.**

	Strain	Efficiency of plating
1	PE577	1.0 ± 0.00
2	PE577 $\Delta ompA$	0.39 ± 0.14
3	PE577 $\Delta ompC$	0.43 ± 0.19
4	PE577 $\Delta ompA, ompC$	0.39 ± 0.07
5	PE577 $\Delta yajC$	0.90 ± 0.18

99  
 100

101 **Supplementary Table 2: DNA Sequences, related to STAR methods.**

	Name	Sequence
1	SPK049	GAAGACCTGGTTGAAGGCGTACG
2	SPK050	GTCAAGGCCGAGCTTCATCG
3	SPK146	CAGCCAGGATCCGAATTCGAGCTCGGCTTAC TCTTGGAGCGAGCAGGTGGTG
4	SPK147	CTTAAGCATTATGCGGCCGCAAGCTTTTAGC CTCCTTGAAGCAGCGCGCGC
5	SPK148	GTATAAGAAGGAGATATACATATGGCGGCAG TATCTTCCCTGACGAAGTTAATC
6	SPK149	GCAGCGGTTTCTTTACCAGACTCGAGTTACA GCATAGTTACGCGTACATAAGC
7	HRP29 Gp47 guideRNA	GGCCCGTCTGGATAACATGCGTTTTAGAGCT AGAAATAGCAAGTTAAAATAAGGCTAGTCCGT TATCAACTTGAAAAAGTGGCACCGAGTCGGT GCTTTTTT
8	HRP29 Gp48 guideRNA	CCGCAGGACCTCGCCTATCGGTTTTAGAGCT AGAAATAGCAAGTTAAAATAAGGCTAGTCCGT TATCAACTTGAAAAAGTGGCACCGAGTCGGT GCTTTTTT

102  
 103  
 104



105 Supplementary table 3: Cryo-EM data collection parameters, related to STAR methods.

EMDB ID	EMD-28227 Virion	EMD-28226 Virion	EMD-28562 tail	EMD-28238 Procapsid
Magnification	53,000	53,000	53,000	64,000
Voltage (keV)	300	300	300	300
Electron exposure (e-/Å <sup>2</sup> )	33	33	33	38.2
Defocus range (µm)	0.8 – 3.0	0.8 – 3.0	0.8 – 3.0	0.8 – 3.0
Pixel size (Å)	0.816	0.816	0.816	0.66
Symmetry imposed	C1	I	C6	I
Number of micrographs	4,489	4,489	4,489	4,167
Final particle images (no.)	33,127	38,666	24,391	60,962
Map resolution (Å)	4.1	3.3	3.3	3.5
FSC threshold	0.143	0.143	0.143	0.143

106

107

108

Supplementary table 4 : Refinement statistics, related to STAR methods.

Model	8ELD		8EM6		8ES4	
Composition (#)						
Chains	13		7		6	
Atoms	20440 (Hydrogens: 0)		15594 (Hydrogens: 0)		17148 (Hydrogens: 3052)	
Residues	Protein: 2738 Nucleotide: 0		Protein: 2128 Nucleotide: 0		Protein: 1841 Nucleotide: 0	
Water	0		0		0	
Ligands	0		0		0	
Bonds (RMSD)						
Length (Å) ( $\sigma > 4\text{\AA}$ )	0.004 (0)		0.002 (0)		0.002 (0)	
Angles ( $^\circ$ ) ( $\sigma > 4\text{\AA}$ )	0.555 (23)		0.499 (12)		0.376 (1)	
MolProbity score	1.98		1.9		2.11	
Clash score	9.35		9.44		20.2	
Ramachandran plot (%)						
Outliers	0		0		0	
Allowed	7.82		5.96		4.5	
Favored	92.18		94.04		95.5	
Rama-Z (Ramachandran plot Z-score, RMSD)						
whole (N = 1821)	-0.95 (0.16)		-0.15 (0.19)		0.53 (0.21)	
helix (N = 432)	1.02 (0.19)		2.28 (0.23)		2.46 (0.26)	
sheet (N = 415)	-0.59 (0.22)		0.60 (0.27)		-0.08 (0.27)	
loop (N = 974)	-1.82 (0.17)		-1.66 (0.18)		-0.39 (0.21)	
Rotamer outliers (%)	0		0		0	
C $\beta$ outliers (%)	0		0		0.06	
Peptide plane (%)						
Cis proline/general	0.0/0.0		0.0/0.0		0.0/0.0	
Twisted proline/general	0.0/0.0		0.0/0.0		0.0/0.0	
CaBLAM outliers (%)	4.21		3.14		1.78	
ADP (B-factors)						
Iso/Aniso (#)	20440/0		15594/0		14096/0	
min/max/mean						
Protein	22.90/70.57/36.57		62.66/181.84/102.87		41.27/169.18/66.95	
Nucleotide	---		---		---	
Ligand	---		---		---	
Water	---		---		---	
Occupancy						
Mean	1		1		1	
occ = 1 (%)	100		100		100	
0 < occ < 1 (%)	0		0		0	
occ > 1 (%)	0		0		0	
Data						
Lengths (Å)	230.11, 184.42, 99.55		151.8, 162.36, 102.96		117.5, 114.24, 298.66	
Angles (Å)	90, 90, 90		90, 90, 90		90, 90, 90	
Supplied Resolution (Å)	3.3		3.5		3.3	
Resolution Estimates (Å)	Masked	Unmasked	Masked	Unmasked	Masked	Unmasked
d FSC (half maps; 0.143)	---	---	---	---	---	---
d 99 (full/half1/half2)	2.9/---/---	2.9/---/---	3.8/---/---	3.6/---/---	3.4/---/---	3.4/---/---
d model	3.2	3.2	3.5	3.6	3.3	3.3
d FSC model (0/0.143/0.5)	---/2.3/3.3	---/2.5/7.6	3.1/3.2/3.6	3.1/3.5/6.0	2.9/3.1/3.4	3.0/3.2/3.8
Map min/max/mean	0.00/0.14/0.00		-0.02/0.06/0.00		-0.07/0.15/0.00	
Model vs. Data						
CC (mask)	0.87		0.81		0.85	
CC (box)	0.56		0.57		0.4	
CC (peaks)	0.56		0.26		0.08	
CC (volume)	0.82		0.81		0.81	
Mean CC for ligands	---		---		---	

110 Relates to Methods sections "Icosahedral and asymmetric image reconstructions of the HRP29  
111 virion", "Icosahedral reconstruction of the HRP29 procapsid", & "Model building and refinement"  
112  
113  
114